Global Integrated Mathematics

https://gim.cultechpub.com/gim

Cultech Publishing

Article

Stability Analysis and Numerical Simulation of a Zika Virus Disease Model with Controls

Emmanuel C. Duru[1,*], Michael C. Anyanwu[1], Godwin C. E. Mbah[2]

[1]Department of Mathematics, Michael Okpara University of Agriculture, Umudike, Nigeria

[2]Department of Mathematics, University of Nigeria, Nsukka, Nigeria

[*]Corresponding author: Emmanuel C. Duru, duru.emmanuel@mouau.edu.ng

Abstract

Zika virus disease is a flavivirus disease transmitted among humans through the bites of infectious Aedes aegypti mosquitoes, through blood transfusions, during sexual intercourse, and during pregnancy. A novel model that incorporates treatment and utilization of Sterile-insect technique as control measures is proposed. This model incorporates the occurrence of asymptomatic cases in the midst of the controls unlike in previous studied considered. Stability analyses show that the zika-free equilibrium point is locally and globally asymptotically stable when the zika control number, R_z, is less than one, and unstable otherwise. A bifurcation analysis was conducted, leveraging the center manifold theorem to ascertain the conditions for stability of the endemic equilibrium point. The effects of the controls considered are demonstrated through the presentation of plots. The findings indicated that the combination of both measures yielded superior outcomes in comparison to the utilization of the controls individually. MATLAB was used for the simulation and plots.

Keywords

Bifurcation, Center-manifold theorem, Endemic equilibrium, Zika virus

2010 AMS: 34D08, 34D20, 34D23, 92B05

Article History

Received: 18 September 2025 Revised: 06 January 2026

Accepted: 26 January 2026 Available Online: 09 February 2026

1. Introduction

Zika virus disease is a zoonotic disease transmitted amongst humans by infectious Aedes aegypti mosquitoes, during pregnancy, blood transfusion and through sex [1,2]. It was first discovered in 1947 in Uganda [1] while the first human cases were reported in 1954 in Nigeria [3]. Common symptoms include headache, maculopapular rash, mild fever, muscle and joint pain, malaise, arthralgia, and conjunctivitis [4,5]. Zika virus disease became a global concern after the first reported infection in pregnant women [6]. Zika infection during pregnancy causes congenital abnormalities of the brain which microcephaly is inclusive [7]. Zika virus also triggers the Guillain-Barre syndrome [8,9]. A report from WHO [10] suggests that information over certain diseases like zika virus disease seem to have been impaired with the onset of COVID-19 pandemic. Zika virus disease has 80% of the cases occurring as asymptomatic and an unclear pathogenesis [11]. Zika virus disease is a zoonosis because non-human primates are reservoirs while humans are incidental hosts [12,13].

The sterile insect technology (SIT) is a pest and insect control mechanism where a large number of sterile males are released to mate with the females in the wild [14,15]. When a sterile male mates with a female, the female can conceive, lay eggs without hatching them [16,17]. SIT was used in northern Mexico to eliminate the Mexican fruit fly and it was used to eliminate tsetse fly in 1997 from Zanzibar [18] and in 2014 from Senegal [19]. Presently, SIT is targeted at eradicating different species of mosquito causing various illnesses [20].

There are many literatures on modelling of zika virus disease such as Andayani et al. [21] who worked on the behaviour of zika virus disease transmission with Beddington-DeAngelis incidence rate in order to determine the endemic conditions of the disease and recovery time. In the research of Olaniyi et al. [22], nonlinear models for the transmission of zika virus disease was formulated. The models incorporated infected mosquitoes, asymptomatic and symptomatic humans. They did the sensitivity analysis to identify the intervention strategies for the disease. González-Parra et al. [23] explored two control strategies to help decrease the spread of the virus in the human and vector populations. They analysed their results with real data obtained from Colombia. SIT was employed to reduce the vector population of the disease and they discovered that introduction of more sterile males into the wild will reduce the population of the mosquitoes with time by Atokolo and Mbah Christopher Ezike [16]. Alshehri and El Hajji [24] worked on a mathematical model for zika virus disease with nonlinear incidence rate. Optimal control analysis using Pontryagin maximum principle was performed to reduce the number of infected humans. They also used a numerical scheme to obtain approximate solution of the system. Alfwzan et al. [25] developed a mathematical model for Zika virus disease which was analysed both numerically and dynamically. Nonstandard numerical methods are employed to check the stability and consistency of solutions. The numerical schemes preserved the behaviour and properties of the model. Ibrahim and Dénes [26] proposed a model for Zika virus disease incorporating mother-to-child and sexual transmission. The model also included a compartment for infants with microcephaly and also showed the impart of asymptomatic humans, seasonality and infection by sexual transmission. They analysed the model considering constant and variable time. Wang et al. [27] worked on a zika virus disease model with transmission by sexual contacts, mosquito bites and sewage. The model was fitted with data from Brazil between 2015-2016. Mosquito bites accounted for large effect of endemicity, followed by transmission through sex and then sewage. Temperature and multiple transmission increased the prevalence of the disease in Brazil as shown in their work. Kouidere et al. [28] proposed a fractional derivative model for an optimal control problem of zika virus disease. Sensitization program against the disease and treatment was employed as controls and it was shown through numerical simulations, how the proposed controls were effective in controlling the spread of the disease. Helikumi et al. [29] developed an optimal control model of zika virus disease incorporating health education campaigns, use of insecticides and preventive measures as controls. Their work showed that the fractional-order model fitted better than the classical integer-order model. The simulation results were seen to justify the use of the controls suggested.

In all the literatures considered, only Atokolo and Mbah Christopher Ezike [16] employed use of sterile insect technique in their modelling analysis. Some researches employed any or combination of treatment, human protection against sexual transmission and mosquito bites as well as destruction of mosquito breeding site as controls. They showed how the controls can reduce the population of mosquitoes [3,21-23,25,27,28]. However, we went further in this new model to show that by controlling the population of mosquitoes as done by Atokolo and Mbah Christopher Ezike [16], the spread of the disease will be controlled. In this work, transmission model for Zika that incorporates the use of SIT and treatment are studied. The model also incorporated occurrence of asymptomatic cases which is one of the major concerns of the disease. The rest of the work is arranged thus; the model describing the disease dynamics, the Zika-free equilibrium point and the basic reproduction number are presented in Section 2; Stability analysis is investigated in Section 3; while in Section 4, numerical simulation is performed and conclusion in Section 5.

2. Mathematical Model

The mathematical model for zika virus disease is made up of six compartments for human population; Susceptible humans S_{h}, Exposed humans E_{hz}, Symptomatic infectious humans $I_{\mathrm{hz}S}$, Asymptomatic infectious humans $I_{\mathrm{hz}A}$, Infectious humans undergoing treatment $I_{\mathrm{hz}T}$, and Recovered humans R_{h} and four compartments for mosquito population; Susceptible mosquitoes S_{zv}, Exposed mosquitoes E_{zv}, Infectious Mosquitoes I_{zv} and the Sterile male mosquitoes, I_{SIT}.

The susceptible human population, S_h is increased by level of recruitment through births and migration and reduced by the rate of movement into the exposed class. The Exposed human population, E_{hz} is increased as more susceptible humans become infected and reduced through by the rate of development of infectiousness. The Symptomatic infectious human population, I_{hzS} is populated by infectious humans who manifest symptoms of the disease while the aymptomatic infectious human population, I_{hzA} is populated by those who do not show any sign of the disease. All the human compartments accounts for natural death while some infectious humans either die naturally or from the disease. Also, some infectious either undergo treatment and recovers while some recover naturally. The susceptible mosquito population, S_{zv} is increased by the level of recruitment and reduced by rate of exposure to the disease and reduction by interaction with sterile males. The SIT mosquitoes are recruited at a rate Λ_s with natural death rate, μ_s. The parameter p represents the proportion of sterile males that will successfully join wild mosquito population [16]. Also, the parameter q accounts for mating competitiveness between SIT mosquitoes and the male Aedes mosquitoes in the environment. The parameter values used for the numerical analysis and simulation were taken from existing literatures such as World health Organization reports, Centre for Disease Protection and Control reports and other literatures from previous modelling analysis. All parameter sources have been properly cited in Table 1 while Figure 1 describes the disease transmission dynamics.

Table 1. Parameters, values and sources.

Parameters	Description	Values	Ref.
Λ_h	Human recruitment rate	50	Assumed
Λ_{zv}	Mosquito recruitment rate	100	Assumed
τ_1	Natural death rate of humans	0.00004	[1]
τ_2	Disease-induced death rate	0.0003	Assumed
μ	Natural death rate of mosquitoes	0.0556	[2]
α	Biting rate of mosquitoes	0.4	[30]
η_1	Probability of transmission from I_{zv} to S_h	0.0009	[1]
η_2	Probability of transmission from I_{hzS} to S_{zv}	0.07	[1]
η_3	Probability of transmission from I_{hzA} to S_{zv}	0.07	[1]
η_4	Probability of transmission from I_{hzT} to S_{zv}	0.05	[31]
δ_2	Incubation rate in humans	0.3333	[2]
ν	Incubation rate in mosquitoes	0.1111	[2]
χ_1	Proportion of infectious humans who are symptomatic	0.31	[31]
χ_2	Proportion of infectious humans who are asymptomatic	0.62	[31]
ω_1	Rate at which I_{hzS} recovers naturally	0.1429	[21]
ω_2	Rate at which I_{hzT} recovers	0.1667	[1]
ω_3	Rate at which I_{hzA} recover	0.118	[2,30]
κ	Mating rate of SIT mosquitoes with Aedes mosquitoes	0.25	[31]
ψ	Rate at which symptomatic infectious humans accept treatment	0.85	[30]

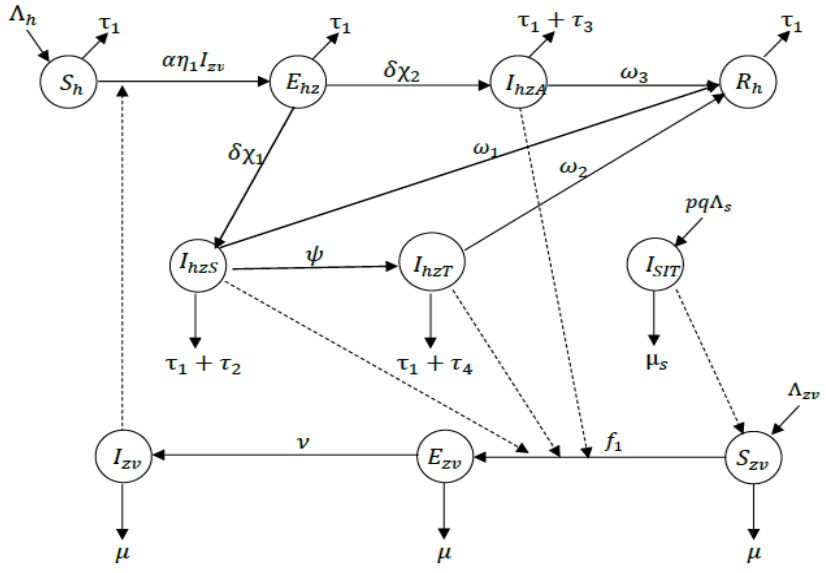

Figure 1. Disease transmission flow.

The model describing the system is:

$$\begin{aligned}
\frac{dS_h}{dt} &= \Lambda_h - (\alpha\eta_1 I_{zv} + \tau_1) S_h, \\
\frac{dE_{hz}}{dt} &= \alpha\eta_1 I_{zv} S_h - \left((\chi_1 + \chi_2)\delta + \tau_1\right) E_{hz}, \\
\frac{dI_{hzS}}{dt} &= \delta\chi_1 E_{hz} - (\tau_1 + \tau_2 + \psi + \omega_1) I_{hzS}, \\
\frac{dI_{hzA}}{dt} &= \delta\chi_2 E_{hz} - (\tau_1 + \tau_3 + \omega_3) I_{hzA}, \\
\frac{dI_{hzT}}{dt} &= \psi I_{hzS} - (\tau_1 + \tau_4 + \omega_2) I_{hzT}, \\
\frac{dR_h}{dt} &= \omega_1 I_{hzS} + \omega_2 I_{hzT} + \omega_3 I_{hzA} - \tau_1 R_h, \\
\frac{dS_{zv}}{dt} &= \Lambda_{zv} - \alpha(\eta_2 I_{hzS} + \eta_3 I_{hzA} + \eta_4 I_{hzT}) S_{zv} - (\kappa I_{SIT} + \mu) S_{zv}, \\
\frac{dE_{zv}}{dt} &= \alpha(\eta_2 I_{hzS} + \eta_3 I_{hzA} + \eta_4 I_{hzT}) S_{zv} - (v + \mu) E_{zv}, \\
\frac{dI_{zv}}{dt} &= v E_{zv} - \mu I_{zv}, \\
\frac{dI_{SIT}}{dt} &= pq\Lambda_s - \mu_s I_{SIT},
\end{aligned} \tag{1}$$

where
$S_h(0)=S_h^0$, $E_{hz}(0)=E_{hz}^0$, $I_{hzS}(0)=I_{hzS}^0$, $I_{hzA}(0)=I_{hzA}^0$, $I_{hzT}(0)=I_{hzT}^0$, $R_h(0)=R_h^0$, $S_{zv}(0)=S_{zv}^0$, $E_{zv}(0)=E_{zv}^0$, $I_{zv}(0)=I_{zv}^0$, $I_{SIT}(0)=I_{SIT}^0$ are the initial conditions for Equation (1).

The solution to Equation (1) lies in the invariant region $\Omega=\Omega_1\times\Omega_2\times\Omega_3$ where

$$\Omega_1=\left\{(S_h,E_{hz},I_{hzS},I_{hzA},I_{hzT},R_h)\in\mathbb{R}_+^6 : N_h\le\frac{\Lambda_h}{\tau_1}\right\}, \tag{2}$$

and

$$\Omega_2=\left\{(S_{zv},E_{zv},I_{zv})\in\mathbb{R}_+^3 : N_{zv}\le\frac{\Lambda_{zv}}{\mu}\right\},\ \Omega_3=\left\{I_{SIT}\in\mathbb{R}_+ \ I_{SIT}\le\frac{pq\Lambda_s}{\mu_s}\right\}, \tag{3}$$

respectively.

2.1 Well-Posedness, Positivity and Boundedness of Solutions

Lemma 1. The solution set $\{S_h(t), E_{hz}(t), I_{hzS}(t), I_{hzA}(t), I_{hzT}(t), R_h(t), S_{zv}(t), E_{zv}(t), I_{zv}(t), I_{SIT}(t)\}$ of Equation (1) with the initial conditions will remain positive $\forall\ t>0$.

Proof.

From Equation (1) we have that

$$\frac{dS_h}{dt}\ge -(\alpha\eta_1 I_{zv}+\tau_1)S_h,$$

$$\frac{dE_{hz}}{dt}\ge -\left((\chi_1+\chi_2)\delta+\tau_1\right)E_{hz},$$

$$\vdots$$

$$\frac{dI_{SIT}}{dt}\ge -\mu_s I_{SIT}.$$

By integration, we have

$$S_h\ge S_h^0 e^{\left\{-\int(\alpha\eta_1 I_{zv}+\tau_1)dt\right\}}>0,$$

$$E_{hz}\ge E_{hz}^0 e^{\left\{-\int((\chi_1+\chi_2)\delta+\tau_1)dt\right\}}>0,$$

$$\vdots$$

$$I_{SIT}\ge I_{SIT}^0 e^{\left\{-\int\mu_s dt\right\}}>0.$$

This shows that the solution to (1) remains positive $\forall\ t>0$.

Lemma 2. The region Ω is positively invariant and is an attractor of all positive solution to the system.

Proof.

The total human and mosquito populations satisfy the differential equations:

$$\begin{aligned}\frac{dN_{\mathrm{h}}}{dt}&=\Lambda_{\mathrm{h}}-\tau_1 N_{\mathrm{h}}-\tau_2(I_{\mathrm{hz}S}+I_{\mathrm{hz}A}+I_{\mathrm{hz}T}),\\ \frac{dN_{zv}}{dt}&=\Lambda_{zv}-\mu I_{zv},\\ \frac{dI_{SIT}}{dt}&=pq\Lambda_s-\mu_s I_{SIT},\end{aligned}\tag{4}$$

respectively.

By Integration, $0\leq N_{\mathrm{h}}\leq\frac{\Lambda_{\mathrm{h}}}{\tau_1}$, $0\leq N_{zv}\leq\frac{\Lambda_{zv}}{\mu}\}$ and $0\leq I_{SIT}\leq\frac{pq\Lambda_s}{\mu_s}$ as $t\to\infty$. Thus, all solutions of Equation (1) are positive and bounded. Lemmas 1 and 2 shows that the model is well-posed epidemiogically, hence can be analysed.

2.2 The Zika Control Number

The disease-free equilibrium point (DFE) of the system which is the steady state of Equation (1) when there is no zika viral infection in the system is given by

$$Z^0=\left(S_{\mathrm{h}}^0, E_{\mathrm{hz}}^0, I_{\mathrm{hz}S}^0, I_{\mathrm{hz}A}^0, I_{\mathrm{hz}T}^0, R_{\mathrm{h}}^0, S_{zv}^0, E_{zv}^0, I_{zv}^0, I_{SIT}^0\right)=\left(\frac{\Lambda_{\mathrm{h}}}{\tau_1},0,0,0,0,0,\frac{\Lambda_{zv}}{\mu},0,0,0\right).$$

The zika control number is a threshold used to measure the average number of new zika infections that will be caused by one index case in an entirely susceptible population. It is denoted in this work by R_z and is derived using the Next-generation matrix approach given in [32,33]. If the zika control number, $R_0<1$ it means that an infected person produces an average of less than one infection, hence the disease will die out from the population with time. The disease class for the system Equation (1) corresponds to;

$$\begin{aligned}\frac{dE_{\mathrm{hz}}}{dt}&=\alpha\eta_1 I_{zv}S_{\mathrm{h}}-\left((\chi_1+\chi_2)\delta+\tau_1\right)E_{\mathrm{hz}},\\ \frac{dI_{\mathrm{hz}S}}{dt}&=\delta\chi_1 E_{\mathrm{hz}}-(\tau_1+\tau_2+\psi+\omega_1)I_{\mathrm{hz}S},\\ \frac{dI_{\mathrm{hz}A}}{dt}&=\delta\chi_2 E_{\mathrm{hz}}-(\tau_1+\tau_2+\omega_3)I_{\mathrm{hz}A},\\ \frac{dI_{\mathrm{hz}T}}{dt}&=\psi I_{\mathrm{hz}S}-(\tau_1+\tau_2+\omega_2)I_{\mathrm{hz}T},\\ \frac{dE_{zv}}{dt}&=\alpha(\eta_2 I_{\mathrm{hz}S}+\eta_3 I_{\mathrm{hz}A}+\eta_4 I_{\mathrm{hz}T})S_{zv}-(v+\mu)E_{zv},\\ \frac{dI_{zv}}{dt}&=vE_{zv}-\mu I_{zv}.\end{aligned}\tag{5}$$

Let $\mathscr{F}$ be the appearance of new infection in Equation (5) and V denote movement into and out of the compartments represented by Equation (5) through any other means, then

$$\mathscr{F}=\begin{bmatrix}\alpha\eta_1 I_{zv}S_{\mathrm{h}}\\0\\0\\0\\\alpha(\eta_2 I_{\mathrm{hz}S}+\eta_3 I_{\mathrm{hz}A}+\eta_4 I_{\mathrm{hz}T})S_{zv}\end{bmatrix}\text{ and }V=\begin{bmatrix}\left((\chi_1+\chi_2)\delta+\tau_1\right)E_{\mathrm{hz}}\\-\delta\chi_1 E_{\mathrm{hz}}+(\tau_1+\tau_2+\psi+\omega_1)I_{\mathrm{hz}S}\\-\delta\chi_2 E_{\mathrm{hz}}+(\tau_1+\tau_2+\omega_3)I_{\mathrm{hz}A}\\(v+\mu)E_{zv}\\-vE_{zv}+\mu I_{zv}\end{bmatrix}.$$

$$\text{Thus, }F=\frac{\partial\mathscr{F}}{\partial Y}=\begin{bmatrix}0&0&0&0&0&C_1\\0&0&0&0&0&0\\0&0&0&0&0&0\\0&0&0&0&0&0\\0&C_2&C_3&C_4&0&0\\0&0&0&0&0&0\end{bmatrix}\text{ and }V=\frac{\partial V}{\partial Y}=\begin{bmatrix}D_1&0&0&0&0&0\\-\chi_1\delta&D_2&0&0&0&0\\-\chi_2\delta&0&D_3&0&0&0\\0&-\psi&0&D_4&0&0\\0&0&0&0&D_5&0\\0&0&0&0&-v&\mu\end{bmatrix},$$

where $C_1=\frac{\alpha\eta_1\Lambda_{\mathrm{h}}}{\tau_1}$, $C_2=\frac{\alpha\eta_2\Lambda_{zv}}{\mu}$, $C_3=\frac{\alpha\eta_3\Lambda_{zv}}{\mu}$, $C_4=\frac{\alpha\eta_4\Lambda_{zv}}{\mu}$, $D_1=(\chi_1+\chi_2)\delta+\tau_1$, $D_2=\tau_1+\tau_2+\psi+\omega_1$, $D_3=\tau_1+\tau_2+\omega_3$, $D_4=\tau_1+\tau_2+\omega_2$, $D_5=v+\mu$. The eigenvalues of the Next-Generation Matrix, FV^{-1} is

$$|FV^{-1}-\lambda I|=\begin{bmatrix}0\\0\\0\\0\\\left(\frac{C_1 v\delta(C_2\chi_1 D_3D_4+C_3\chi_2 D_2D_4+C_4\chi_1\psi D_3)}{\mu D_1D_2D_3D_4D_5}\right)^{\frac{1}{2}}\\-\left(\frac{C_1 v\delta(C_2\chi_1 D_3D_4+C_3\chi_2 D_2D_4+C_4\chi_1\psi D_3)}{\mu D_1D_2D_3D_4D_5}\right)^{\frac{1}{2}}\end{bmatrix}.$$

The zika control number is the dominant eigenvalue of $|FV^{-1}-\lambda I|$ and is given by

$$R_z=\left(\frac{C_1\nu\delta(C_2\chi_1D_3D_4+C_3\chi_2D_2D_4+C_4\chi_1\psi D_3)}{\mu D_1D_2D_3D_4D_5}\right)^{\frac{1}{2}}. \tag{6}$$

The proportion, $\frac{C_1\nu\delta C_2\chi_1}{\mu D_1D_2D_5}$ in R_z gives the total expected infections at the DFE point by one symptomatic infectious human, $\frac{C_1\nu\delta C_3\chi_2}{\mu D_1D_3D_5}$ gives the total expected infections at the DFE point by one asymptomatic infectious human while $\frac{C_1\nu\delta C_4\chi_1\psi}{\mu D_1D_2D_4D_5}$ gives the total expected infections at the DFE point by one infectious human undergoing treatment.

3. Analysis of Equilibria

3.1 Local Stability of the Disease-Free Equilibrium Point

Theorem 1. The disease-free equilibrium point is locally asymptotically stable (LAS) if $R_z<1$ and unstable if otherwise.

Proof.

To determine the nature of the stability of the DFE point, the system, Equation (1) is linearized around the DFE point, Z^0 to obtain the eigenvalues of the system. If all the eigenvalues are negative then, the DFE point is LAS, otherwise it is unstable.

Let the right-hand side of Equation (1) be denoted as

$$\begin{aligned}
f_1&=\Lambda_h-(\alpha\eta_1I_{zv}+\tau_1)S_h,\\
f_2&=\alpha\eta_1I_{zv}S_h-\big((\chi_1+\chi_2)\delta+\tau_1\big)E_{hz},\\
f_3&=\delta\chi_1E_{hz}-(\tau_1+\tau_2+\psi+\omega_1)I_{hzS},\\
f_4&=\delta\chi_2E_{hz}-(\tau_1+\tau_2+\omega_3)I_{hzA},\\
f_5&=\psi I_{hzS}-(\tau_1+\tau_2+\omega_2)I_{hzT},\\
f_6&=\omega_1I_{hzS}+\omega_2I_{hzT}+\omega_3I_{hzA}-\tau_1R_h,\\
f_7&=\Lambda_{zv}-\alpha(\eta_2I_{hzS}+\eta_3I_{hzA}+\eta_4I_{hzT})S_{zv}-(\kappa I_{SIT}+\mu)S_{zv},\\
f_8&=\alpha(\eta_2I_{hzS}+\eta_3I_{hzA}+\eta_4I_{hzT})S_{zv}-(\nu+\mu)E_{zv},\\
f_9&=\nu E_{zv}-\mu I_{zv},\\
f_{10}&=pq\Lambda_s-\mu_sI_{SIT},
\end{aligned} \tag{7}$$

The Jacobian, J of Equation (7) evaluated at the DFE point, Z^0 is given by

$$J(Z^0)=\begin{bmatrix}
-\tau_1 & 0 & 0 & 0 & 0 & 0 & 0 & 0 & -C_1 & 0\\
0 & -D_1 & 0 & 0 & 0 & 0 & 0 & 0 & C_1 & 0\\
0 & \delta\chi_1 & -D_2 & 0 & 0 & 0 & 0 & 0 & 0 & 0\\
0 & \delta\chi_2 & 0 & -D_3 & 0 & 0 & 0 & 0 & 0 & 0\\
0 & 0 & \psi & 0 & -D_4 & 0 & 0 & 0 & 0 & 0\\
0 & 0 & \omega_1 & \omega_3 & \omega_2 & -\tau_1 & 0 & 0 & 0 & 0\\
0 & 0 & -C_2 & -C_3 & -C_4 & 0 & -\mu & 0 & 0 & \frac{\kappa\Lambda_{zv}}{\mu}\\
0 & 0 & C_2 & C_3 & C_4 & 0 & 0 & -D_5 & 0 & 0\\
0 & 0 & 0 & 0 & 0 & 0 & 0 & \nu & -\mu & 0\\
0 & 0 & 0 & 0 & 0 & 0 & 0 & 0 & 0 & -\mu_s
\end{bmatrix},$$

where all the $C_i's$ and $D_i's$ are same as in Section 2.2. The eigenvalues of the Jacobian matrix, $J(Z^0)$ corresponds to these diagonal elements, $(-\tau_1, -\tau_1, -\mu, -\mu_s)$ which are all negative and the eigenvalues of the Jacobian submatrix, $J_1(Z^0)$ given by

$$J_1(Z^0)=\begin{bmatrix}
-D_1 & 0 & 0 & 0 & 0 & C_1\\
\chi_1\delta & -D_2 & 0 & 0 & 0 & 0\\
\chi_2\delta & 0 & -D_3 & 0 & 0 & 0\\
0 & \psi & 0 & -D_4 & 0 & 0\\
0 & C_2 & C_3 & C_4 & -D_5 & 0\\
0 & 0 & 0 & 0 & \nu & \mu
\end{bmatrix}.$$

The Jacobian submatrix is derived by deleting any column with one entry with its corresponding row. The eigenvalues of the Jacobian submatrix correspond to the root of its characteristic polynomial given by

$$P(\lambda)=Q_0\lambda^6+Q_1\lambda^5+Q_2\lambda^4+Q_3\lambda^3+Q_4\lambda^2+Q_5\lambda+Q_6 \tag{8}$$

where

$Q_0=1$,

$Q_1=D_1+D_2+D_3+D_4+D_5+\mu$,

$Q_2=D_1(D_2+D_3+D_4+D_5)+D_2\ (D_3+D_4+D_5)+D_3(D_4+D_5)+D_4D_5+\mu(D_1+D_2+D_3+D_4+D_5)$,

$Q_3=D_1D_2(D_3+D_4+D_5)+D_1D_3(D_4+D_5)+D_1D_4D_5+D_2D_3(D_4+D_5)+\mu D_3D_4$

$+D_4D_5(D_2+D_3)+\mu D_1(D_2+D_3+D_4+D_5)+\mu D_5(D_3+D_4)+\mu D_2(D_3+D_4+D_5)$

$Q_4=\mu D_1(D_2D_3+D_2D_4+D_3D_4+D_4D_5)+\mu D_2(D_3D_4+D_3D_5+D_4D_5)+\mu D_3D_4D_5$

$+D_1D_2(D_3D_4+D_3D_5+D_4D_5)+D_1D_3D_4D_5+\frac{C_1v\delta(C_3\chi_2D_2D_4+C_2\chi_1D_3D_4)}{D_2D_3}$

$+D_2D_3D_4D_5+\frac{C_1v\delta C_4\chi_1\psi(D_2+D_3)}{D_2D_4}+\mu D_1D_2D_5[1-R_z^2]+\mu D_1D_3D_5[1-R_z^2]$,

$Q_5=D_2D_3D_4[\mu D_1+\mu D_5+D_1D_5]+\frac{C_1v\delta\chi_1D_3(C_2D_4+C_4\psi)}{D_2}+\mu D_1D_3D_4D_5[1-R_z^2]$

$+\frac{C_1v\delta(C_3\chi_2D_2D_4D_4+C_4\chi_1\phi D_3D_3)}{D_3D_4D_5}+\mu D_1D_2D_4D_5[1-R_z^2]+\mu D_1D_2D_3D_5[1-R_z^2]$,

$Q_6=\mu D_1D_2D_3D_4D_5[1-R_z^2]$.

Applying Descartes rules of signs [34], we will see that there will be no sign changes in our polynomial if $R_z<1$ and if there are no sign changes, then all the roots of the polynomial which corresponds to the eigenvalues of the Jacobian submatrix, J_1 will be negative. Thus, the DFE of Equation (1) will be LAS if $R_z<1$. Therefore, the DFE point of the system (1) is LAS when $R_z<1$.

3.2 Global Stability of the Disease-Free Equilibrium Point

Theorem 2. Consider the system of differential equations

$$\frac{dX}{dt}=F_1(X,0), \tag{9}$$

$$\frac{dY}{dt}=F_2(X,Y),F_2(X,0)=0, \tag{10}$$

where Equation (9) is the sub-system of Equation (1), satisfied by non-disease class, $X=(S_h,R_h,S_{zv},I_{SIT})$ and Equation (10) is the sub-system of Equation (1) satisfied by the disease class, $Y=(E_{hz},I_{hzS},I_{hzA},I_{hzT},E_{zv},I_{zv})$. The DFE, Z^0 is globally asymptotically stable (GAS) if Equation (9) is GAS, and if in (10), $BX_2-F_2(X,Y)\geq 0$, where B is the Jacobian matrix of $J_1(X,Y)$, evaluated at Z^0 and $F_2(X,Y)$ is the right-hand side of the system associated with the disease class.

Proof.

From the system Equation (1), solving the differential equations of $X=(S_h,R_h,S_{zv},I_{SIT})$ at the DFE point gives

$$\begin{aligned} S_h&=\frac{\Lambda_h}{\tau_1}+\left(S_h^0-\frac{\Lambda_h}{\tau_1}\right)e^{-\tau_1 t},\\ R_h&=R_h^0e^{-\tau_1 t},\\ S_{zv}&=\frac{\Lambda_{zv}}{\mu}+\left(S_{zv}^0-\frac{\Lambda_{zv}}{\mu}\right)e^{-\tau_1 t},\\ I_{SIT}&=\frac{pq\Lambda_s}{\mu_s}+\left(I_{SIT}^0-\frac{pq\Lambda_s}{\mu_s}\right)e^{-\tau_1 t}. \end{aligned} \tag{11}$$

As $t\to\infty$, we will have $S_h\to\frac{\Lambda_h}{\tau_1}$, $R_h\to 0$, $S_{zv}\to\frac{\Lambda_{mv}}{\mu}$ and $I_{SIT}\to\frac{pq\Lambda_s}{\mu_s}$ respectively which are the values of (S_h,R_h,S_{zv},I_{SIT}) at the DFE point.

Also, the matrix B is given by

$$B=\begin{bmatrix} -D_1 & 0 & 0 & 0 & 0 & C_1\\ \chi_1\delta & -D_2 & 0 & 0 & 0 & 0\\ \chi_2\delta & 0 & -D_3 & 0 & 0 & 0\\ 0 & \psi & 0 & -D_4 & 0 & 0\\ 0 & C_2 & C_3 & C_4 & -D_5 & 0\\ 0 & 0 & 0 & 0 & v & \mu \end{bmatrix}$$

and $BX_2-F_2(X,Y)=\begin{bmatrix} \alpha\eta_1\left(\frac{\Lambda_h}{\tau_1}-S_h\right)I_{zv} \\ 0 \\ 0 \\ 0 \\ \alpha\left(\frac{\Lambda_{zv}}{\mu}-S_{zv}\right)(\eta_2 I_{hzS}+\eta_3 I_{hzA}+\eta_4 I_{hzT}) \\ 0 \end{bmatrix}$.

It is obvious to see that $S_h(t)\leq\frac{\Lambda_h}{\tau_1}$ and $S_{zv}(t)\leq\frac{\Lambda_{zv}}{\mu}$. Hence, we are certain of non-negativity of all the rows in the matrix showing that $BX_2-F_2(X,Y)\geq 0$ is satisfied. Hence, the DFE point is GAS.

3.3 Endemic Equilibrium Point of the System

The Zika endemic equilibrium point, (ZEEP) of the system is the state where zika virus disease persist in the system. At the ZEEP denoted in this work by $Z^*=(S_h^*, E_{hz}^*, I_{hzS}^*, I_{hzA}^*, I_{hzT}^*, R_h^*, S_{zv}^*, E_{zv}^*, I_{zv}^*, I_{SIT}^*)\backslash\backslash)$, the state variables are expressed in the form;

$S_h^*=\frac{\Lambda_h}{\alpha\eta_1 I_{zv}^*+\tau_1}$, $E_{hz}^*=\frac{\alpha\eta_1 I_{zv}^* S_h^*}{(\chi_1+\chi_2)\delta+\tau_1}$, $I_{hzS}^*=\frac{\delta\chi_1 E_{hz}^*}{\tau_1+\tau_2+\psi+\omega_1}$, $I_{hzA}^*=\frac{\delta\chi_2 E_{hz}^*}{\tau_1+\tau_2+\omega_3}$, $I_{hzT}^*=\frac{\psi I_{hzS}^*}{\tau_1+\tau_2+\omega_2}$, $R_h=\frac{\omega_1 I_{hzS}^*+\omega_2 I_{hzT}^*+\omega_3 I_{hzA}^*}{\tau_1}$,

$S_{zv}^*=\frac{\Lambda_{zv}}{\alpha\left(\eta_2 I_{hzS}^*+\eta_3 I_{hzA}^*+\eta_4 I_{hzT}^*\right)+\left(\kappa I_{SIT}^*+\mu\right)}$,

$E_{zv}^*=\frac{\alpha\left(\eta_2 I_{hzS}^*+\eta_3 I_{hzA}^*+\eta_4 I_{hzT}^*\right)}{v+\mu}$, $I_{zv}^*=\frac{vE_{zv}^*}{\mu}$ and $I_{SIT}^*=\frac{pq\Lambda_s}{\mu_s}$ which corresponds to the system of equations;

$0=\Lambda_h-\left(\alpha\eta_1 I_{zv}^*+\tau_1\right)S_h^*$,

$0=\alpha\eta_1 I_{zv}^* S_h^*-\left((\chi_1+\chi_2)\delta+\tau_1\right)E_{hz}^*$,

$0=\delta\chi_1 E_{hz}^*-(\tau_1+\tau_2+\psi+\omega_1)I_{hzS}^*$,

$0=\delta\chi_2 E_{hz}^*-(\tau_1+\tau_2+\omega_3)I_{hzA}^*$,

$0=\psi I_{hzS}^*-(\tau_1+\tau_2+\omega_2)I_{hzT}^*$,

$0=\omega_1 I_{hzS}^*+\omega_2 I_{hzT}^*+\omega_3 I_{hzA}^*-\tau_1 R_h^*$,

$0=\Lambda_{zv}-\alpha\left(\eta_2 I_{hzS}^*+\eta_3 I_{hzA}^*+\eta_4 I_{hzT}^*\right)S_{zv}^*-\left(\kappa I_{SIT}^*+\mu\right)S_{zv}^*$,

$0=\alpha\left(\eta_2 I_{hzS}^*+\eta_3 I_{hzA}^*+\eta_4 I_{hzT}^*\right)S_{zv}^*-(v+\mu)E_{zv}^*$,

$0=vE_{zv}^*-\mu I_{zv}^*$,

$0=pq\Lambda_s-\mu_s I_{SIT}^*$,

Thus, substituting expressions for these state variables:

$(S_h^*, I_{hzS}^*, I_{hzA}^*, I_{hzT}^*, R_h^*, S_{zv}^*, E_{zv}^*, I_{zv}^*, I_{SIT}^*)$, into E_{hz}^* where applicable yields

$$H_1 E_{hz}^{*2}+H_2 E_{hz}^*=0 \qquad (12)$$

where $H_1=\left[\frac{D_1\Lambda_{zv}}{\mu}+\frac{\mu\Lambda_h D_1 D_5}{C_1 v}\right]R_z^2$ and $H_2=\Lambda_h\left[\frac{\kappa pq\Lambda_s}{\mu_s}+\mu(1-R_z^2)\right]$ respectively.

The trivial solution $E_{hz}^*=0$ gives the disease-free equilibrium point already proven to be locally and globally asymptotically stable when $R_z<1$. Applying Descartes rules of signs in Equation (12), we will see that there will be no sign changes in our polynomial if $R_z<1$ and if there are no sign changes, then all roots of Equation (12) will be negative. But there is a possibility of obtaining a positive root from Equation (12) if $R_z>1$ and $H_2<0$. Hence, a unique endemic equilibrium is guaranteed to exist only when $R_z>1$.

3.4 Bifurcation Analysis

The method of Castillo-Chavez and Song [35] based on the Center manifold theorem is used to carry out bifurcation analysis to determine if the zika-endemic equilibrium point is LAS or not. From the theorem [35], given

$q=\sum_{\{k,i,j\}}^{n} v_k w_i w_j \frac{\partial^2 f_k(0,0)}{\partial y_i \partial y_j}$,

$r=\sum_{k,i}^{n} v_k w_i \frac{\partial^2 f_k(0,0)}{\partial y_i \partial \psi}$.

then, if $q<0$ and $r>0$, then a forward bifurcation occurs at $\psi=0$ and if $q>0$, $r>0$, a backward bifurcation occurs at $\psi=0$.

Proof.

Let η_1^* be the bifurcation parameter, then $R_z=1$ implies that

$1=\frac{\alpha\eta_1\Lambda_h v\delta(C_2\chi_1 D_3 D_4 + C_3\chi_2 D_2 D_4 + C_4\chi_1\psi D_3)}{\tau_1\mu D_1 D_2 D_3 D_4 D_5}$.

Setting $\eta_1=\eta_1^*$ and making it the subject of the formula, we will have

$\eta_1^* = \frac{\tau_1\mu D_1 D_2 D_3 D_4 D_5}{\alpha\Lambda_h v\delta(C_2\chi_1 D_3 D_4 + C_3\chi_2 D_2 D_4 + C_4\chi_1\psi D_3)}$.

Let $J(Z^0,\eta_1^*)$\) be the Jacobian matrix of $f(x,\eta_1^*)$ at the zika-free equilibrium Z^0. The matrix $J(Z^0,\eta_1^*)$ possesses a zero eigenvalue, while the remaining eigenvalues have negative real part. Therefore, $J(Z^0,\eta_1^*)$ is non-hyperbolic, and [35] can be applied to analyze the dynamics of the model around the bifurcation parameter η_1^*. The right eigenvector $\overline{w}=(w_1,w_2,w_3,...,w_{10})^T$ and the left eigenvector $\overline{v}=(v_1,v_2.v_3,...,v_{10})^T$ corresponding to the zero eigenvalues satisfy the systems $J\left(Z^0,\eta_1^*\right)\overline{w}=0$ and $\overline{v}J(Z^0,\eta_1^*)=0$.

Here, the Jacobian matrix $J\left(Z^0,\eta_1^*\right)$ and $J(Z^0)$ are only different in C_1^* where η_1 is replaced with η_1^*. So, we will have

$$J\left(Z^0,\eta_1^*\right)\overline{w}=\begin{pmatrix} -\tau_1\omega_1-C_1^*\,\omega_9 \\ -D_1\omega_2+C_1^*\,\omega_9 \\ D_6\omega_2-D_2\omega_3 \\ D_7\omega_2-D_3\omega_4 \\ \psi\omega_3-D_4\omega_5 \\ w_1\omega_3+w_2\omega_5+w_3\omega_4-\tau_1\omega_6 \\ -C_2\omega_3-C_3\omega_4-C_4\omega_5-\mu\omega_7-\frac{\kappa\Lambda_{zv}\omega_{10}}{\mu} \\ C_2\omega_3+C_3\omega_4+C_4\omega_5-D_5\omega_8 \\ v\omega_8-\mu\omega_9 \\ -\mu_s\omega_{10} \end{pmatrix}=0.$$

Taking $w_2=1>0$ so that the other terms can be easily obtained in terms of w_2 as follows:

$w_1=-\frac{D_1 w_2}{\tau_1}$, $w_3=\frac{D_6 w_2}{D_2}$, $w_4=\frac{D_7 w_2}{D_3}$, $w_5=\frac{\psi D_6 w_2}{D_2 D_4}$, $w_6=\frac{(\omega_1 D_3 D_4 D_6+\omega_2\psi D_3 D_6+\omega_3\tau_1 D_2 D_4 D_7)w_2}{\tau_1 D_2 D_3 D_4}$,

$w_7=-\frac{(C_2 D_3 D_4 D_6+C_4\psi D_3 D_6+C_3 D_2 D_4 D_7)w_2}{\mu D_2 D_3 D_4}$, $w_8=\frac{\mu D_1 w_2}{C_1^* v}$, $w_9=\frac{D_1 w_2}{C_1^*}$, $w_{10}=0$.

Using the Jacobian matrix, $J\left(Z^0,\eta_1^*\right)$ and the vector $\overline{v}$, then

$$\overline{v}J\left(Z^0,\eta_1^*\right)=\begin{pmatrix} -v_1\tau_1 \\ -v_2 D_1+v_3 D_6+v_4 D_7 \\ -v_3 D_2+v_5\psi+v_6\omega_1-v_7 C_2+v_8 C_2 \\ -v_4 D_3+v_6\omega_3-v_7 C_3+v_8 C_3 \\ -v_5 D_4+v_6\omega_2-v_7 C_4+v_8 C_4 \\ -v_6\tau_1 \\ -v_7\mu \\ -v_8 D_5+v_9 v \\ -v_1 C_1^*+v_2 C_1^*-v_9\mu \\ -\frac{v_7\kappa\Lambda_{zv}}{\mu}-v_{10}\mu_s \end{pmatrix}=0.$$

The result of the product $\overline{v}J\left(Z^0,\eta_1^*\right)$ taking $v_2=1>0$ so that the other terms can be easily obtained in terms of v_2 is given as follows;

$v_1=v_6=v_7=v_{10}=0$, $v_3=\frac{v_2 vC_1^*(C_4+D_4)}{\mu D_4 D_5}$, $v_4=\frac{v_2 vC_1^* C_3}{\mu D_3 D_5}$, $v_5=\frac{v_2 vC_1^* C_4}{\mu D_4 D_5}$, $v_8=\frac{v_2 vC_1^*}{\mu D_5}$, $v_9=\frac{v_2 C_1^*}{\mu}$.

We make these useful notations; $S_h=y_1$, $E_{hz}=y_2$, $I_{hzS}=y_3$, $I_{hzA}=y_4$, $I_{hzT}=y_5$, $R_h=y_6$, $S_{zv}=y_7$, $E_{zv}=y_8$, $I_{zv}=y_9$ and $I_{SIT}=y_{10}$. for ease of identification. Also, let

$$\begin{bmatrix} f_1 \\ f_2 \\ f_3 \\ f_4 \\ f_5 \\ f_6 \\ f_7 \\ f_8 \\ f_9 \\ f_{10} \end{bmatrix} = \begin{bmatrix} \Lambda_h - (\alpha\eta_1 y_9 + \tau_1)y_1 \\ \alpha\eta_1 y_9 y_1 - \big((\chi_1+\chi_2)\delta+\tau_1\big)y_2 \\ \delta\chi_1 y_2 - (\tau_1+\tau_2+\psi+\omega_1)y_3 \\ \delta\chi_2 y_2 - (\tau_1+\tau_3+\omega_3)y_4 \\ \psi y_3 - (\tau_1+\tau_4+\omega_2)y_5 \\ \omega_1 y_3 + \omega_2 y_5 + \omega_3 y_4 - \tau_1 y_6 \\ \Lambda_{zv} - \alpha(\eta_2 y_3 + \eta_3 y_5 + \eta_4 y_4)y_7 - (\kappa y_{10}+\mu)y_7 \\ \alpha(\eta_2 y_3 + \eta_3 y_5 + \eta_4 y_4)y_7 - (\nu+\mu)y_8 \\ \nu y_8 - \mu y_9 \\ pq\Lambda_s - \mu_s y_{10} \end{bmatrix}.$$

Thus, we will have

$$\frac{\partial^2 f_1}{\partial y_1 \partial y_9} = -\alpha\eta_1^*, \ \frac{\partial^2 f_1}{\partial y_9 \partial y_1} = \alpha\eta_1^*, \ \frac{\partial^2 f_7}{\partial y_7 \partial y_3} = -\alpha\eta_2, \ \frac{\partial^2 f_7}{\partial y_7 \partial y_4} = -\alpha\eta_3, \ \frac{\partial^2 f_7}{\partial y_7 \partial y_5} = -\alpha\eta_4, \backslash]$$

$$\frac{\partial^2 f_8}{\partial y_3 \partial y_7} = \alpha\eta_2, \ \frac{\partial^2 f_8}{\partial y_7 \partial y_4} = \alpha\eta_3, \ \frac{\partial^2 f_8}{\partial y_7 \partial y_5} = \alpha\eta_4, \ \frac{\partial^2 f_2}{\partial y_1 \partial \eta_1^*} = \alpha I_{zv}, \ \frac{\partial^2 f_2}{\partial y_9 \partial \eta_1^*} = \alpha y_1.$$

The summations for q with $\bar{v}$ and $\bar{w}$ now becomes

$$q = v_2 \sum_{i,j}^{n} w_i w_j \frac{\partial^2 f_2(0,0)}{\partial y_i \partial y_j} + v_8 \sum_{i,j}^{n} w_i w_j \frac{\partial^2 f_8(0,0)}{\partial y_i \partial y_j}$$

$$= 2v_2 w_1 w_9 \frac{\partial^2 f_2(0,0)}{\partial y_1 \partial y_9} + 2v_8 w_3 w_7 \frac{\partial^2 f_8(0,0)}{\partial y_3 \partial y_7} + 2v_8 w_7 w_4 \frac{\partial^2 f_8(0,0)}{\partial y_7 \partial y_4} + 2v_8 w_7 w_5 \frac{\partial^2 f_8(0,0)}{\partial y_7 \partial y_5}$$

$$= -\frac{2D_1^2 w_2^2 v_2 \alpha\eta_1^*}{\tau_1 C_1^*} - \frac{2D_6 w_2^2 v v_2 \alpha\eta_2 C_1^* D_1 R_z^2}{\mu C_1 D_2} - \frac{2D_7 w_2^2 v v_2 C_1^* \alpha\eta_4 D_1 R_z^2}{\mu C_1 D_3} - \frac{2\psi D_6 w_2^2 v v_2 C_1^* \alpha\eta_3 D_1 R_z^2}{\mu C_1 D_2 D_4}.$$

Since all the parameters in q are all positive, then $q<0$. We then proceed to find r.

Similarly, the summations for r now becomes

$$r = v_1 \sum_{i}^{n} w_i \frac{\partial^2 f_1(0,0)}{\partial y_i \partial \eta_1^*} + v_2 \sum_{i}^{n} w_i \frac{\partial^2 f_2(0,0)}{\partial y_i \partial \eta_1^*}.$$

From the values of $v_i^{'}s$, $v_1=0$. Therefore, r becomes

$$r = \frac{v_2 \sum_{i}^{n} w_i \partial^2 f_2(0,0)}{\partial y_i \partial \eta_1^*}.$$

Hence, we will have

$$r = v_2 w_1 \frac{\partial^2 f_2(0,0)}{\partial y_1 \partial \eta_1^*} + v_2 w_9 \frac{\partial^2 f_2(0,0)}{\partial y_9 \partial \eta_1^*} = -\frac{v_2 D_1 w_2 \alpha y_9}{\tau_1} + \frac{v_2 D_1 w_2 \alpha y_1}{C_1^*}$$

$$= \frac{v_2 D_1 w_2 \alpha \left[y_1 \tau_1 - y_9 C_1^* \right]}{\tau_1 C_1^*}.$$

The parameter, $r>0$ if $y_1\tau_1 > y_9 C_1^*$. Thus, the system given by Equation (1) will experience forward bifurcation if $r>0$ since $q<0$. If $r \nsucc 0 \backslash)$, then backward bifurcation occurs in the system. Therefore, the zika endemic equilibrium will be LAS if $r>0$ and unstable if otherwise.

3.5 Global Stability of Zika Endemic Equilibrium Point

The method of Lyapunov given in the works of [36,37] is used to check if the zika endemic equilibrium point is globally asymptotically stable or not. Lyapunov methods are robust, general and can handle complex systems, hence, more suitable for nonlinear and continuous systems. Consider a Lyapunov function of the form;

$$V = \frac{1}{2} \bar{Y}^2, \tag{13}$$

where $\bar{Y} = (S_h + E_{hZ} + I_{hzS} + I_{hzA} + I_{hzT} + R_h + S_{zv} + E_{zv} + I_{zv} + I_{SIT})$.

Then,

$$\frac{dV}{dt}=\bar{Y}\,\dot{\bar{Y}}, \tag{14}$$

where $\dot{\bar{Y}}=\left(\dot{S}_h+\dot{E}_h+\dot{I}_{hzS}+\dot{I}_{hzA}+\dot{I}_{hzT}+\dot{R}_h+\dot{S}_{zv}+\dot{E}_{zv}+\dot{I}_{zv}+\dot{I}_{SIT}\right)$.

Equation (14) becomes

$$\begin{aligned}\frac{dV}{dt}&=\bar{Y}(\dot{S}_h+\dot{E}_h+\dot{I}_{hzS}+\dot{I}_{hzA}+\dot{I}_{hzT}+\dot{R}_h+\dot{S}_{zv}+\dot{E}_{zv}+\dot{I}_{zv}+\dot{I}_{SIT})\\&=\bar{Y}(\Lambda_h-(\alpha\eta_1 I_{zv}+\tau_1)S_h+\alpha\eta_1 I_{zv}S_h-\left((\chi_1+\chi_2)\delta+\tau_1\right)E_{hz}+\delta\chi_1 E_{hz}\\&\quad-(\tau_1+\tau_2+\psi+\omega_1)I_{hzS}+\delta\chi_2 E_{hz}-(\tau_1+\tau_3+\omega_3)I_{hzA}+\psi I_{hzS}\\&\quad-(\tau_1+\tau_4+\omega_2)I_{hzT}+\omega_1 I_{hzS}+\omega_2 I_{hzT}+\omega_3 I_{hzA}-\tau_1 R_h+\Lambda_{zv}\\&\quad-\alpha(\eta_2 I_{hzS}+\eta_3 I_{hzA}+\eta_4 I_{hzT})S_{zv}-(\kappa I_{SIT}+\mu)S_{zv}+\alpha(\eta_2 I_{hzS}+\eta_3 I_{hzA}+\eta_4 I_{hzT})S_{zv}-(v+\mu)E_{zv}+vE_{zv}-\mu I_{zv}+pq\Lambda_s-\mu_s I_{SIT}\\&=\bar{Y}(\Lambda_h-\tau_1(S_h+E_{hz}+I_{hzS}+I_{hzA}+I_{hzT}+R_h)-\tau_2 I_{hzS}-\tau_3 I_{hzA}-\tau_4 I_{hzT}\\&\quad+\Lambda_{zv}-\mu(S_{zv}+E_{zv}+I_{zv})-\kappa I_{SIT}S_{zv}+pq\Lambda_s-\mu_s I_{SIT})\\&=\bar{Y}(\Lambda_h-\tau_1 N_h-\tau_2 I_{hzS}-\tau_3 I_{hzA}-\tau_4 I_{hzT}+\Lambda_{zv}-\mu N_{zv}-\kappa I_{SIT}S_{zv}+pq\Lambda_s\\&\quad-\mu_s I_{SIT}).\end{aligned}$$

Clearly, $0\le N_h\le\frac{\Lambda_h}{\tau_1}$, $0\le N_{zv}\le\frac{\Lambda_{zv}}{\mu}$ and $0\le I_{SIT}\le\frac{pq\Lambda_s}{\mu_s}$ as shown in section (1), which means that $\tau_1 N_h\le\Lambda_h$, $\mu N_{zv}\le\Lambda_{zv}$ and $\mu_s I_{SIT}\le pq\Lambda_s$. Using $\tau_1 N_h=\Lambda_h$, $\mu N_{zv}=\Lambda_{zv}$ and $\mu_s I_{SIT}=pq\Lambda_s$, then

$$\frac{dV}{dt}=-(\tau_2 I_{hzS}+\tau_3 I_{hzA}+\tau_4 I_{hzT}+\kappa I_{SIT}S_{zv})\bar{Y}<0.$$

This shows that the zika endemic equilibrium point is GAS since $\frac{dV}{dt}<0$. The global stability of the zika endemic equilibrium point indicates that zika virus disease will persist in the system at a stable level irrespective of the size of the initial infected population. This necessitates the need for the control measures suggested in this work.

4. Numerical Simulation

4.1 Effects of SIT Only

The purpose of releasing the sterile males is for them to mate with the wild females so that the females when pregnant will lay eggs but cannot hatch them. The effects of this interaction are shown in Figures 2-3 using the values in Table 1. The simulation showed that the infectious human and mosquito populations reduced greatly as the sterile males mates with the females in the wild. This occurrence is associated with the fact that when the females in the wild mates with the sterile males and become pregnant, the lay eggs without hatching them. This causes the number of the mosquitoes to reduce with time.

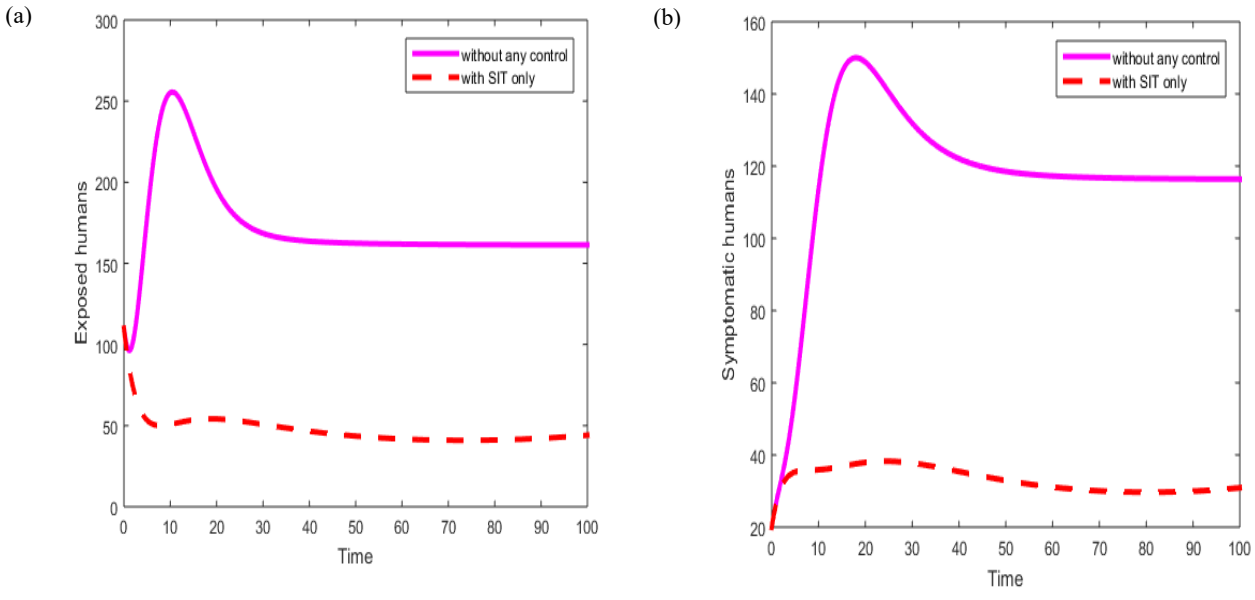

Figure 2. Exposed and symptomatic humans under SIT. (a) Exposed humans under SIT only. (b) Symptomatic humans under SIT only.

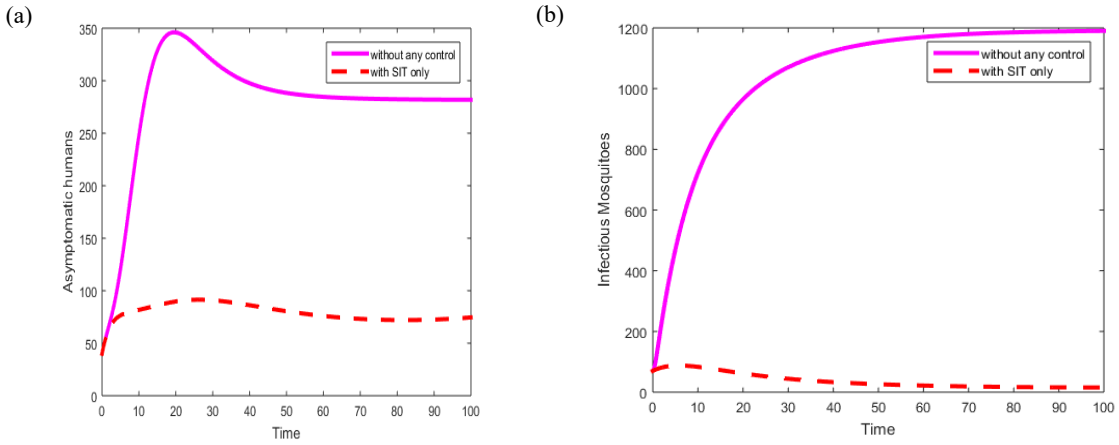

Figure 3. Asymptomatic humans and infectious mosquitoes under SIT. (a) Asymptomatic humans under SIT only. (b) Infectious mosquitoes under SIT only.

4.2 Effects of Treatment Only

In Figures 4-5, the effects of using treatment only as a control measure is shown. The plots showed that while the population of symptomatic humans reduced significantly under treatment, the other infectious compartments were not much affected. The symptomatic humans reduced as expected since they are the only population undergoing treatment. However, the occurrence of asymptomatic cases who are not treated ensures that zika virus disease will continue to spread in the system explaining why the other infectious compartment did not reduce significantly. This observation underscores the need for preventive measure to be adopted in the control of the disease since treatment offers little help in this regard.

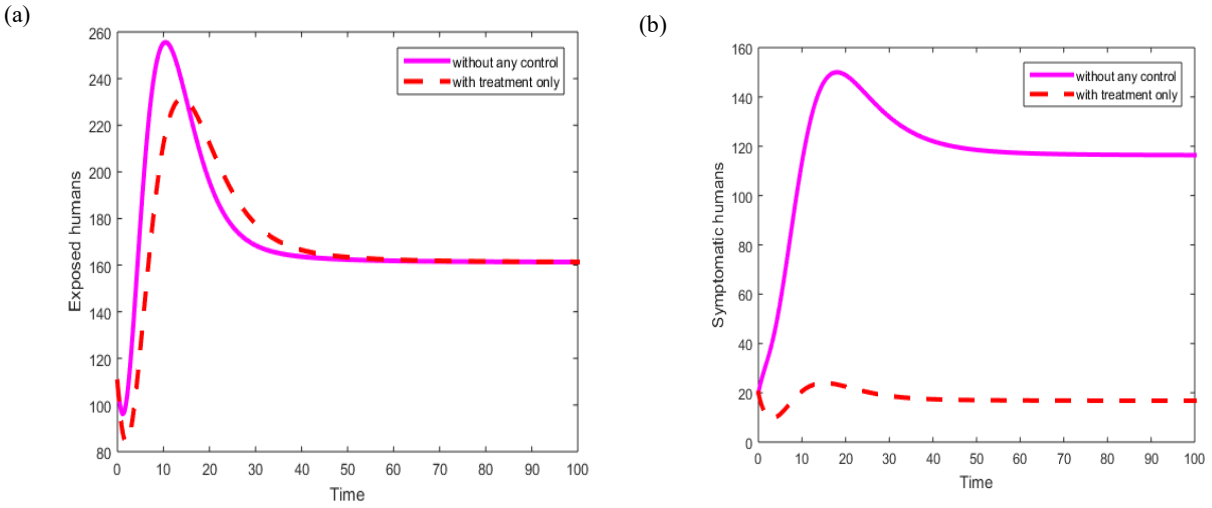

Figure 4. Exposed and symptomatic humans under treatment only. (a) Exposed humans under treatment only. (b) Symptomatic humans under treatment only.

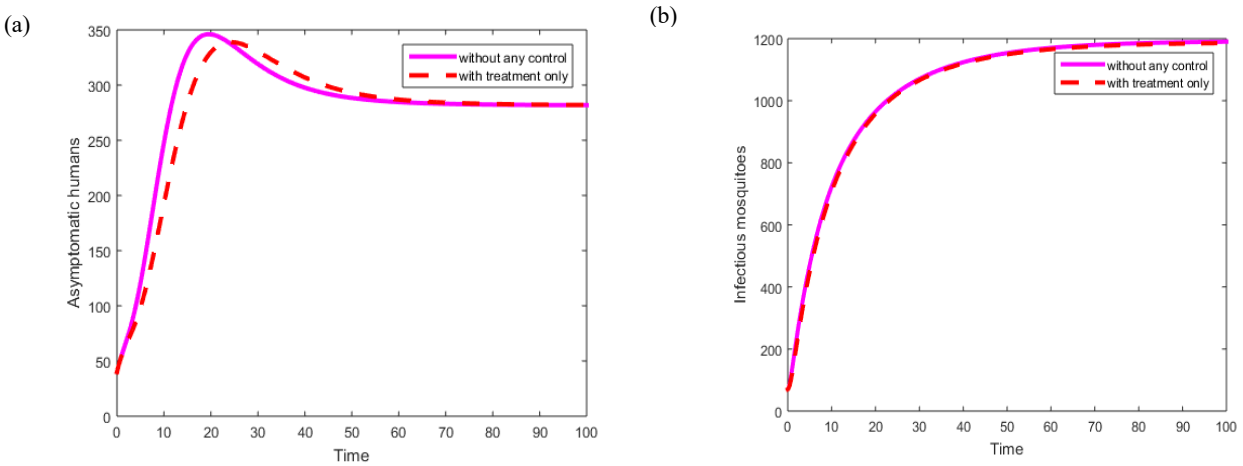

Figure 5. Asymptomatic humans and infectious mosquitoes under treatment only. (a) Asymptomatic humans under treatment only. (b) Infectious mosquitoes under treatment only.

4.3. Effects of Treatment and SIT

In this case, the effect of combining both control measures are simulated and shown in Figures 6-7. This control measure is shown to perform better than using either of the controls separately. Both the infectious human and infectious mosquito populations reduced more significantly in this scenario than using when any of the controls are employed independently. This shows that it is preferably to employ measures that affect humans and mosquitoes in the control of the disease than using a measure that affect only either of them. The results of the simulation confirm existing knowledge that controlling the multiplication of mosquitoes is a significant step towards controlling disease borne by mosquitoes.

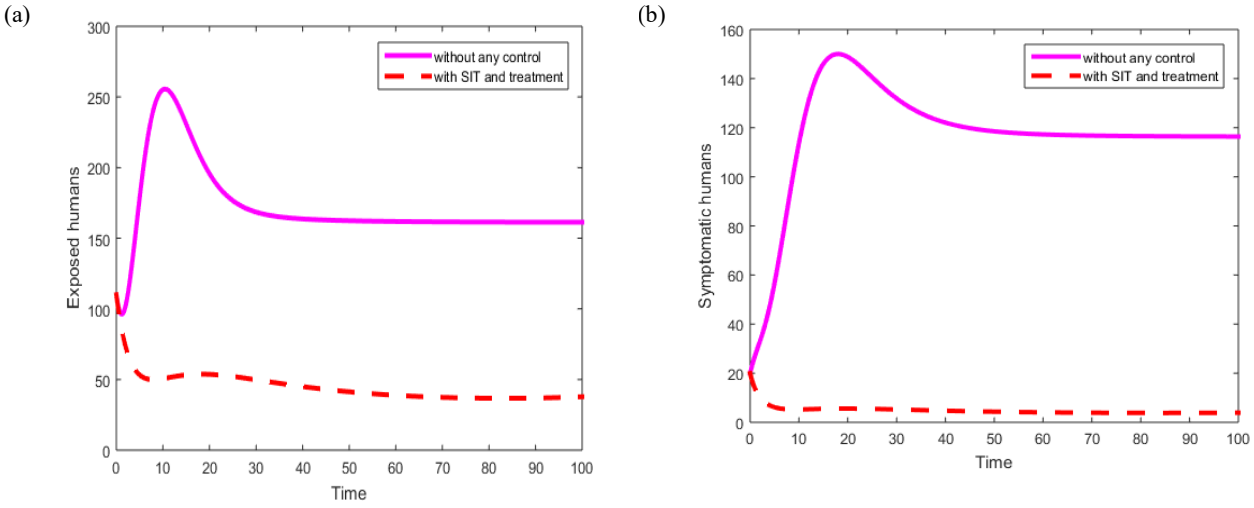

Figure 6. Exposed and symptomatic humans under SIT and treatment. (a) Exposed humans under SIT and treatment. (b) Symptomatic humans under SIT and treatment.

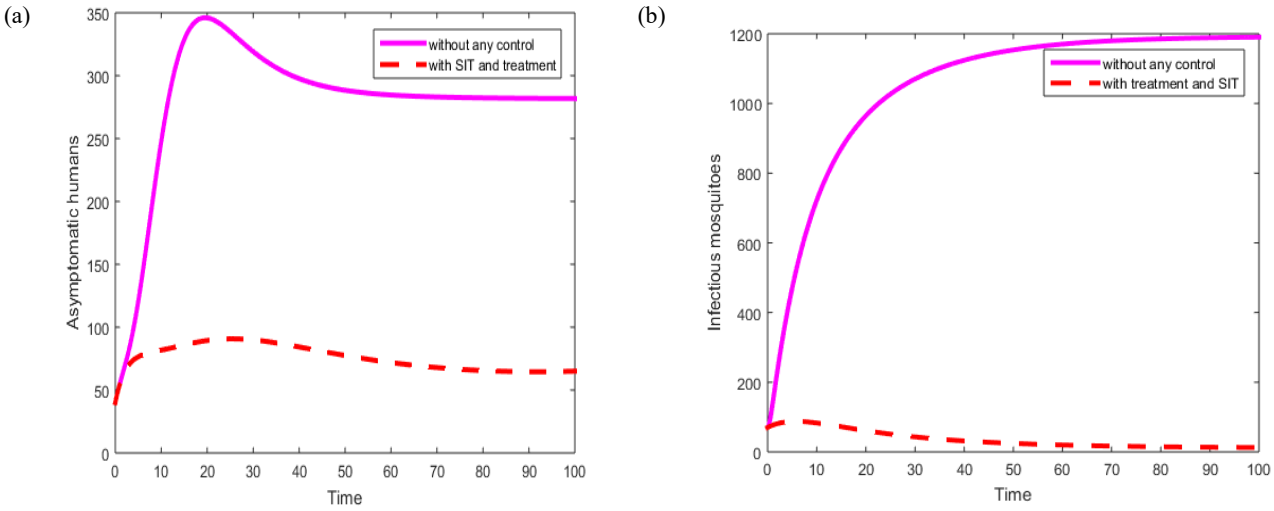

Figure 7. Asymptomatic humans and infectious mosquitoes under SIT and treatment. (a) Asymptomatic humans under SIT and treatment. (b) Infectious mosquitoes under SIT and treatment.

5. Sensitivity Analysis of the Zika Model

Sensitivity analysis was carried out in this work using the normalized forward sensitivity index [30]. Let p be any parameter then, the sensitivity index of R_z with respect to p is given by

$$\mathcal{Y}_p^{R_z} = \frac{\partial R_z}{\partial p} \times \frac{p}{R_z}. \tag{15}$$

The sensitivity indices are shown in Figures 8-9 and Table 2. The parameters with positive sensitivity indices increase the endemicity of zika virus disease hence there is need to reduce their values in order to effectively control the disease. On the other hand, the parameters with negative sensitivity indices decrease the endemicity of zika virus disease and need to be increased to help control the disease. From Table 2, the contact rate of mosquitoes with humans, α has the highest sensitivity index. This shows that one of the ways to control the spread of zika virus is to reduce or eliminate the contact rate of humans with mosquitoes. The more humans have contact with mosquitoes, the higher the probability of infections taking place. Also, the rate of recruitment of humans and mosquitoes also increase the endemicity of the disease.

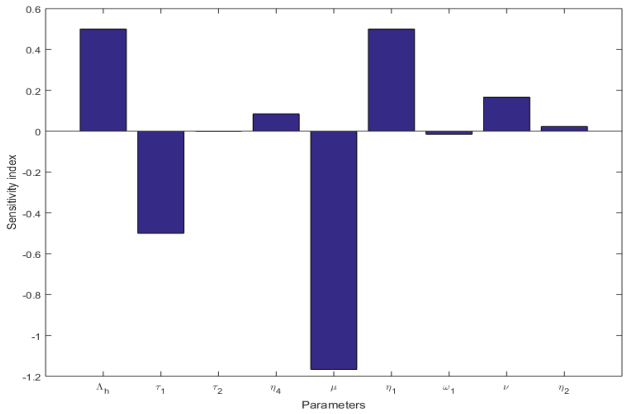

Figure 8. Sensitivity plot.

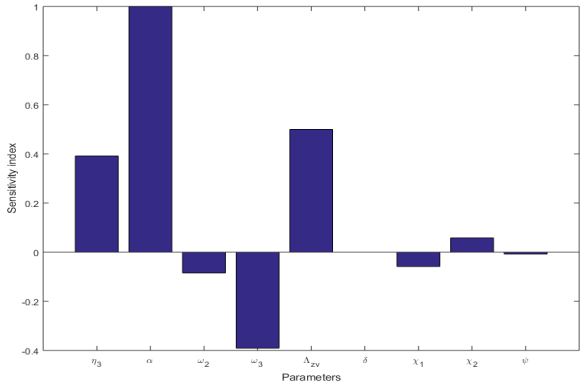

Figure 9. Sensitivity plot cont'd.

Table 2. Sensitivity indices for R_z.

Parameter	Values	Sensitivity Index	Parameter	Values	Sensitivity Index
Λ_h	50	0.5	τ_1	0.00004	-0.5002
Λ_{zv}	100	0.5	τ_2	0.0003	-0.00003
α	0.4	1	τ_3	0.0002	-0.00007
δ	0.3333	0.00007	τ_4	0.0001	-0.00005
η_1	0.0009	0.5	χ_1	0.31	-0.0585
η_2	0.07	0.0233	χ_2	0.62	0.0585
η_3	0.07	0.3918	ω_1	0.1429	-0.0156
η_4	0.05	0.0848	ω_2	0.1667	-0.0847
v	0.1111	0.1668	ω_3	0.118	-0.3917
ψ	0.85	-0.0077	μ	0.0556	-1.1668

This implies that humans must avoid places where mosquitoes are rampant and ensure that efforts are made to reduce the recruitment of mosquitoes. It is also shown that probabilities of transmission, η_i, i=1,2,3, incubation rates, δ and v, as well as asymptomatic cases all increase the endemicity of the disease. The parameters with negative sensitivity index such as rates of recovery, ω_i, i=1,2,3, natural death rate of mosquitoes, μ, rate of treatment, ψ, etc. need to be increased to help reduce the spread of the disease.

The 3D plots further highlighting the effects of the parameters on the zika control number are shown in Figures 10-12. In Figure 10, it is shown that while an increase in the proportion of symptomatic cases, χ_1 leads to a decrease in the zika control number, R_0, an increase in the proportion of asymptomatic cases, χ_2 leads to an increase in the zika control number. Also, an increase in human contact rate with mosquitoes, α leads to an increase in the zika control number, R_0, as well as an increase in the probability of transmission from mosquitoes to humans, η_1. However, in Figure 11, an increase in incubation rates of the disease both in human and mosquito populations, δ, v, and probabilities of transmission from humans to mosquitoes, η_2, η_3 all lead to an increase in the zika control number. But, in Figure 12, it is shown that an increase in η_4 leads to an increase in the zika control number, R_0 while an increase in the rate of treatment, ψ leads to a decrease in the zika control number. This further explain the sensitivity analysis in Table 2 and Figures 8-9, thus highlighting key parameters that affect the endemicity of the disease.

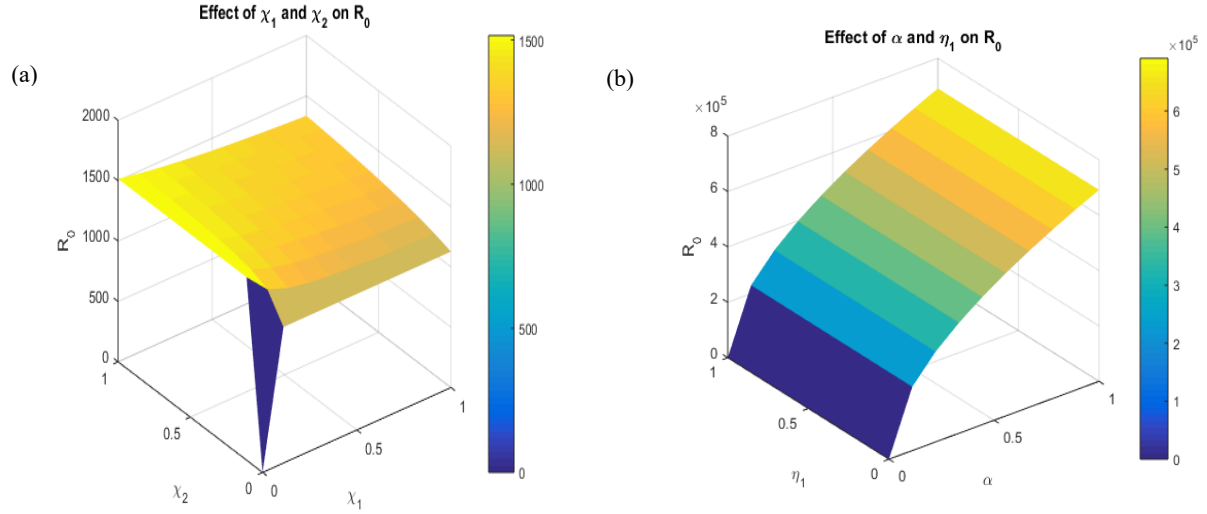

Figure 10. Sensitivity of the zika control number R_0 with respect to the parameters χ_1, χ_2 and α, η_1. (a) 3D plot of R_0 w.r.t χ_1 and χ_2. (b) 3D plot of R_0 w.r.t α and η_1.

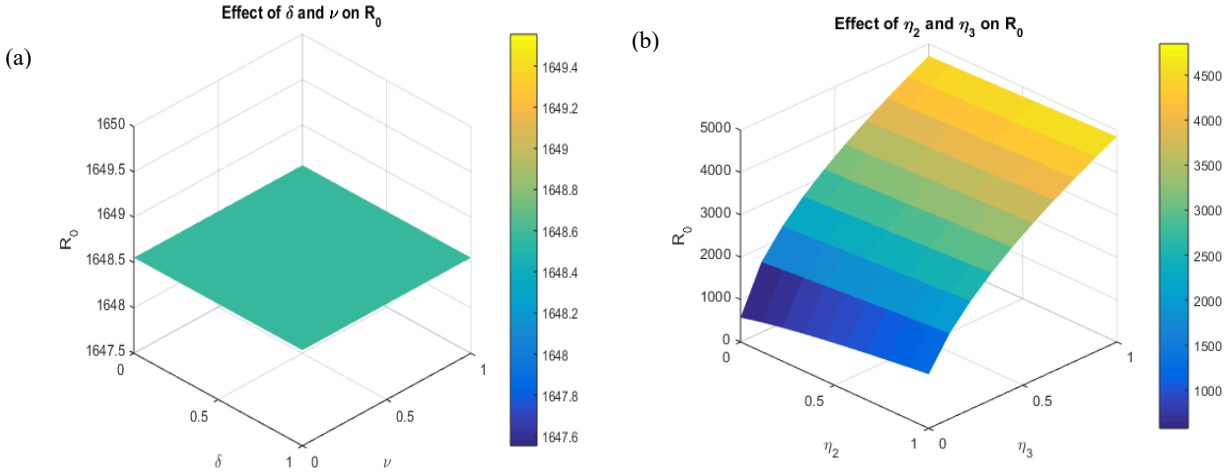

Figure 11. Sensitivity of the zika control number R_0 with respect to the parameters δ, v and η_2, η_3. (a) 3D plot of R_0 w.r.t δ and v. (b) 3D plot of R_0 w.r.t η_2 and η_3.

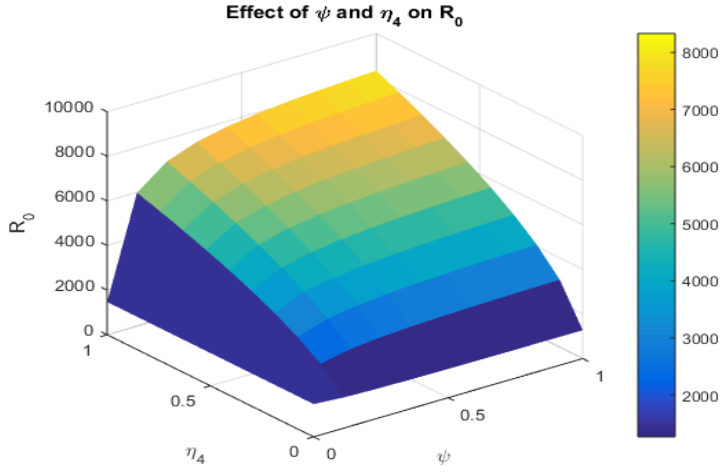

Figure 12. Sensitivity of the zika control number R_0 with respect to the parameters ψ, η_4.

5. Conclusions

This work considers a zika virus disease model which incorporated treatment of infectious humans and vector control through sterile insect technique. The model is set up to show how the interaction of female mosquitoes in the wild and the introduced sterile males leads to control of zika virus disease. The DFE point of the model is shown to be both locally and globally asymptotically stable when the zika control number, R_z is less than one. The existence of a unique endemic equilibrium was shown and stability conditions of the endemic state were also obtained. The vector population

was effectively reduced by the application of SIT hence the spread of the disease will be reduced with time. The effect of treatment was also shown in the work. The analysis showed that employing treatment alone in the control of zika virus disease is not a good strategy due to increased rate of asymptomatic occurrence associated with the disease. Conclusively, employing SIT and treatment simultaneously will help to control the Aedes mosquito population and spread of the disease as shown in this work. In furtherance of this research, other control measures can be investigated and compared with the ones employed here. Also, considering saturated incidence in the force of infection or application of further controls will help understand the disease dynamics more.

Conflict of Interest

The authors declare no conflict of interest.

Generative AI Statement

The authors declare that no Generative AI was used in the creation of this manuscript.

References

[1] Lamwong J, Pongsumpun P. Age structural model of Zika virus. International Journal Modeling and Optimization, 2018, 8, 17-23.
[2] Anyanwu MC, Mbah GC, Duru EC. On mathematical model for zika virus disease control with wolbachia-infected mosquitoes. Abacus Mathematics Science Series, 2020, 47, 35.
[3] Rakkiyappan R, Latha VP, Rihan FA. A fractional-order model for zika virus infection with multiple delays. Complexity, 2019, 2019(1), 4178073. DOI: 10.1155/2019/4178073
[4] World Health Organization. The history of zika virus. 2016. Available from: https://www.who.int/news-room/feature-stories/detail/the-history-of-zika-virus (accessed on 20 May 2025).
[5] Centre for Disease Control and Protection. Zika symptoms and complications. 2025. Available from: https://www.cdc.gov/zika/signs-symptoms/index.html (accessed on 2 August 2025).
[6] Mysorekar IU, Diamond MS. Modeling Zika virus infection in pregnancy. New England Journal of Medicine, 2016, 375(5), 481-484. DOI: 10.1056/NEJMcibr16054450
[7] Calvet G, Aguiar RS, Melo AS, Sampaio SA, de Filippis I, Fabri A, et al. Detection and sequencing of Zika virus from amniotic fluid of fetuses with microcephaly in Brazil: A case study. The Lancet Infectious Diseases, 2016, 16(6), 653-660. DOI: 10.1016/S1473-3099(16)00095-5
[8] Krauer F, Riesen M, Reveiz L, Oladapo OT, Martínez-Vega R, Porgo TV, et al. Zika virus infection as a cause of congenital brain abnormalities and Guillain-Barré syndrome: Systematic review. PLoS Medicine, 2017, 14(1), e1002203. DOI: 10.1371/journal.pmed.1002203
[9] Boret SE, Escalante R, Villasana M. Mathematical modelling of zika virus in Brazil. 2021. Available from: https://hal.archives-ouvertes.fr/hal-03505850 (accessed on 20 May 2025).
[10] World Health Organization. Countries and territories with current or previous Zika virus transmission. 2023. Available from: https://www.who.int/publications/m/item/countries-and-territories-with-current-or-previous-zika-virus-transmission (accessed on 2 August 2025).
[11] Goswami NK, Srivastav AK, Ghosh M, Shanmukha B. Mathematical modeling of zika virus disease with nonlinear incidence and optimal control. InJournal of Physics: Conference Series, 2018, 1000, 012114. DOI: 10.1088/1742-6596/1000/1/012114
[12] Musso D, Roche C, Robin E, Nhan T, Teissier A, Cao-Lormeau VM. Potential sexual transmission of Zika virus. Emerging Infectious Diseases, 2015, 21(2), 359-361. DOI: 10.3201/eid2102.141363
[13] Vue D, Tang Q. Zika virus overview: Transmission, origin, pathogenesis, animal model and diagnosis. Zoonoses, 2021, 1(1). DOI: 10.15212/ZOONOSES-2021-0017
[14] Vreysen MJ, Robinson AS, Hendrichs J. Area-wide control of insect pests: From research to field implementation. Springer, 2007. DOI: 10.1007/978-1-4020-6059-5
[15] Dyck VA, Hendrichs J, Robinson AS. Sterile insect technique: principles and practice in area-wide integrated pest management. Taylor & Francis, 2021. Available from: https://library.oapen.org/handle/20.500.12657/101482 (accessed on 20 May 2025).
[16] Atokolo W, Mbah Christopher Ezike G. Modeling the control of zika virus vector population using the sterile insect technology. Journal of Applied Mathematics, 2020, 2020(1), 6350134. DOI: 10.1155/2020/6350134
[17] Anguelov R, Dumont Y, Lubuma J. Mathematical modeling of sterile insect technology for control of anopheles mosquito. Computers & Mathematics with Applications, 2012, 64(3), 374-389. DOI: 10.1016/j.camwa.2012.02.068
[18] UN FAO. Expert group confirms: Tsetse fly eradicated on zanzibar. 1997. Available from: https://www.iaea.org/newscenter/pressreleases/expert-group-confirms-tsetse-fly-eradicated-zanzibar (accessed on 20 May 2025).
[19] UN FAO. Senegal nears first victory in war on tsetse fly. 2014. Available from: https://www.fao.org/newsroom/detail/Senegal-nears-first-victory-in-war-on-tsetse-fly/en (accessed on 20 May 2025).
[20] Chen LH, Hamer DH. Zika virus: Rapid spread in the western hemisphere. Annals of Internal Medicine, 2016, 164(9), 613-615. DOI: 10.7326/M16-0150
[21] Andayani P, Sari LR, Suryanto A, Darti I. Numerical study for ZIKA virus transmission with Beddington-Deangelis incidence rate. Far East Journal of Mathematical Sciences (FJMS), 2019, 111(1), 145-157. DOI: 10.17654/MS111010145
[22] Olaniyi SJ. Dynamics of Zika virus model with nonlinear incidence and optimal control strategies. Applied Mathematics & Information Sciences, 2018, 12(5), 969-982. DOI: 10.18576/amis/120510
[23] González-Parra G, Díaz-Rodríguez M, Arenas AJ. Optimization of the controls against the spread of Zika virus in populations. Computation, 2020, 8(3), 76. DOI: 10.3390/computation8030076

[24] Alshehri A, El Hajji M. Mathematical study for Zika virus transmission with general incidence rate. AIMS Math, 2022, 7(4), 7117-7142. DOI: 10.3934/math.2022397
[25] Alfwzan WF, Raza A, Martin-Vaquero J, Baleanu D, Rafiq M, Ahmed N, et al. Modeling and transmission dynamics of Zika virus through efficient numerical method. AIP Advances, 2023, 13(9). DOI: 10.1063/5.0168945
[26] Ibrahim MA, Dénes A. A mathematical model for Zika virus infection and microcephaly risk considering sexual and vertical transmission. Axioms, 2023, 12(3), 263-288. DOI: 10.3390/axioms12030263
[27] Wang L, Jia Q, Zhu G, Ou G, Tang T. Transmission dynamics of Zika virus with multiple infection routes and a case study in Brazil. Scientific Reports, 2024, 14(1), 7424. DOI: 10.1038/s41598-024-58025-7
[28] Kouidere A, El Bhih A, Minifi I, Balatif O, Adnaoui K. Optimal control problem for mathematical modeling of Zika virus transmission using fractional order derivatives. Frontiers in Applied Mathematics and Statistics, 2024, 10, 1376507. DOI: 10.3389/fams.2024.1376507
[29] Helikumi M, Lolika PO, Makau KA, Ndambuki MC, Mhlanga A. Modeling Zika virus disease dynamics with control strategies. InInformatics, 2024, 11(4), 85. DOI: 10.3390/informatics11040085
[30] Duru EC, Mbah GC, Anyanwu MC, Nnamani NT. Modelling the co-infection of malaria and zika virus disease. Journal of the Nigerian Society of Physical Sciences, 2024, 1938. DOI: 10.46481/jnsps.2024.1938
[31] Duru EC, Mbah GC, Uzoma A. Numerical simulations and solutions of a mathematical model for Zika virus disease. Applications of Modelling and Simulation, 2025, 9, 139-153. Available from: https://arqiipubl.com/ojs/index.php/AMS_journal/article/view/835 (accessed on 20 May 2025).
[32] Van den Driessche P, Watmough J. Reproduction numbers and sub-threshold endemic equilibria for compartmental models of disease transmission. Mathematical Biosciences, 2002, 180(1-2), 29-48. DOI: 10.1016/S0025-5564(02)00108-6
[33] Diekmann O, Heesterbeek JA, Roberts MG. The construction of next-generation matrices for compartmental epidemic models. Journal of the Royal Society Interface, 2010, 7(47),873-885. DOI: 10.1098/rsif.2009.0386
[34] Wang X. A simple proof of Descartes's rule of signs. The American Mathematical Monthly, 2004, 111(6), 525-526. DOI: 10.1080/00029890.2004.11920108
[35] Castillo-Chavez C, Song B. Dynamical models of tuberculosis and their applications. Mathematical Biosciences & Engineering, 2004, 1(2), 361-404. DOI: 10.3934/mbe.2004.1.361
[36] Mpande L, Kajunguri D, Mpolya E. Modeling and stability analysis for measles metapopulation model with vaccination. Applied Computation and Mathematics, 2015, 4(6), 431-444. DOI: 10.11648/j.acm.20150406.16
[37] Ozioko AL, Aja RO, Abang SI, Atokolo W, Ahmane QO, Mbah GC. The dynamics of Nipah virus (NiV) transmission and analysis. Journal of Mathematics and Computer Science, 2023, 31, 367-391. DOI: 10.22436/jmcs.031.04.03